A GFPE Method To Estimate Noise Levels From Aircraft Departures At Montijo Aerodrome

Diogo Alexandre Neves Carreira Mendes
diogo.mendes@tecnico.ulisboa.pt
Instituto Superior Técnico, Universidade de Lisboa, Portugal

December 2020

Abstract

In the past years, consciousness about health and environment are forcing each day to restrict the maximum allowed noise levels at the cities and big urban areas, leading to more accurate noise prediction tools that can include a much bigger number of parameters that influence the propagation itself as well as achieve a more complex propagation model with less computational demand and which is more user friendly, promoting this way that further developments can be made faster and better.
This dissertation work starts by presenting the fundamentals of acoustic physics, and then the used numerical method that predict the sound propagation in the atmosphere as well as its limitations.
The main goal of this thesis is to study the sound propagation in the atmosphere produced by an aircraft's departure from Montijo's airport and to use a numerical application which allows to incorporate the variance in the source position with some of the parameters that were used in the C language program which perform the calculations.
In order to achieve so, it was elaborated a Matlab script that generate the inputs of the executable and allows to obtain the noise levels for different situations of interest, accordingly to ANP database procedures for aircraft departures within the flight path suggested by the NAV-Portugal.

Keywords: sound propagation, SPL, GFPE, NPD, acoustic, noise, atmosphere

1. Introduction

Humanity is living in a world with permanent contact with noise, remaining each day less places on Earth where we are totally free from undesirable sounds. Noise can frustrate and impede speech communication and it can represent a physical health hazard as well since the exposure to high noise levels can cause permanent hearing loss besides depression and anxiety.

In the last years, society's growing environmental and health conscience has leaded the national authorities to reinforce existing legislation concerning the maximum permissible noise levels. Towards the described context, the knowledge of the sound propagation assumes a growing importance.

Nowadays all the previous studies associated with the construction of new infrastructures or the renewing of another ones, that can generate significant levels of noise, namely airports, evolves the need for count-

less studies, which take into account an incredible amount of parameters in order to achieve precise results. In this scope, there has been a continuos effort to decrease aircraft noise emissions through specified planning of procedures for the flight paths allowed in the vinicity of airports.

The existent methods to calculate the sound level in a given atmosphere, have different degrees of complexity, accuracy and speed. Some of them do not incorporate many parameters that influence the real atmospheric sound behavior or are computationally inefficient. As proven in previous studys [3], the GFPE method is the most suitable one to study sound propagation in the atmosphere. Using this method, it was developed in previous studys a computational program in C language to calculate the sound field between a sourcer and a receiver, where it's included several inputs that represent the most significant parameters of sound propagation phenomena. This method puts together the best accuracy and computational effort of each of the existing methods and its results were validated by comparison to well known benchmark results.

Finally, in order to apply the sound propagation to a real case scenario, it was developed a Matlab program in which is calculated an aircraft departure trajectory following the ECAC Vol.II procedures along the flight path suggested by NAV-Portugal.

2. Theoretical Fundamentals

Sound is a mechanical wave, which is an oscillation of pressure transmitted through a medium, composed of frequencies within the range of hearing and with a level sufficiently strong to be felt by human eardrums and that ultimately results in listening.

Sound pressure in a atmosphere is the local pressure deviation from the average atmospheric pressure caused by a sound wave. The sound pressure level (SPL) is a logarithmic measure of the effective sound pressure of a sound relative to a reference value. Its value is measured in decibel and is given by the following equation,

$$L_P = 10log_{10}\left(\frac{1}{2}\frac{|p_c^2|}{p_{ref}^2}\right) \tag{1}$$

It is also useful for benchmarking purposes to define another parameter called Sound Transmission Loss [9] which is a quantification in decibels of how much energy is prevented from traveling through a medium and it can be obtained by,

$$STL = 10log_{10}\frac{|p_c|^2}{|p_{free}|^2_{r=1}} \tag{2}$$

Where $|p_{free}|^2_{r=1}$ is the sound pressure from a direct acoustic field at 1 meter from the source.

2.1. Homogeneous Atmosphere

In a homogeneous atmosphere with no wind neither boundaries or surfaces, sound propagation is strictly axisymmetric and there is no angle dependence.It is also assumed that average density and pressure remain constant and therefore the sound wave propagation is influenced by three main cases:

1 - Acoustic spreading - The sound wave travels from a source with an increasing radius through distance,where the sound intensity decreases as the surface of the wave front expands. The resulting dissipation is dependent on the propagation distance and independent of frequency.

2 - Atmospheric absorption - As sound waves pass through the atmosphere, they lose energy in a gradual process that depends on air temperature, humidity and also atmospheric pressure. Air absorption attenuates high frequency components faster than low frequency ones and this is why the sound from distant traffic or jets usually have a low rumbling character.

3 - Ground absorption - The proximity to a ground surface results in a complex interaction between the sound waves causing local cancellation of direct and ground-reflected

sound waves. Considering an aircraft flying situation where it is not bounded by any ground surfaces, there are still sound waves that reach the ground, where part of each is reflected to the air and other part absorbed by the ground.

2.2. Inhomogeneous Atmosphere

Acoustical propagation direction is largely affected by wind gradients as well as temperature gradients. Regarding wind effect, when it blows from the receiver to the source direction, it makes the sound waves to bend upwards from the ground. This create a zone of quiet at large distances, and this zone it is called sound shadow. When the wind blows in the same direction as the sound, sound waves are bended downwards, which can increase significantly the level of noise reaching distant receivers [4].

Regarding temperature gradients, they produce similar bending effects. During daytime conditions, when usually air is warmer near the ground, sound is bent upwards away from the ground which under calm conditions may cause sounds shadows in all directions from the source.

In this thesis it will be incorporated the effect of atmospheric refraction, which means that the sound speed in the atmosphere depends on temperature, where higher temperature yields faster sound propagation. The sound speed expression is presented below.

$$c = c_0\sqrt{\frac{T}{T_0}} \tag{3}$$

3. GFPE Formulation

3.1. Inhomogeneous Helmholtz equation

Considering a monopole source in a moving atmosphere with a non constant sound speed profile, the corresponding three dimensional Helmholtz equation is

$$k_{eff}^2\nabla.(k_{eff}^{-2}\nabla.p_c) + k_{eff}^2\nabla p_c = 0 \tag{4}$$

As the majority of sound propagation models is based on a two-dimensional atmosphere, further simplifications may be applied to the three dimensional Helmholtz equation, obtaining the following expression

$$\frac{1}{r}\frac{d}{dr}(r\frac{dp_c}{dr})+k_{eff}^2\frac{d}{dz}(k_{eff}^{-2}\frac{dp_c}{dz})+\frac{1}{r^2}\frac{d^2p_c}{d\phi^2}+k_{eff}^2p_c=0 \tag{5}$$

In the axisymmetric simplification we consider that the sound field is independent of the azimuthal angle and therefore we can neglect the third term on the left-hand side of the previous equation while assuming the far-field approximation, where the resulting equation is

$$\frac{d^2q_c}{dr^2} + k_{eff}^2\frac{d}{dz}(k_{eff}^{-2}\frac{dq_c}{dz}) + k_{eff}^2q_c = 0 \tag{6}$$

For most numerical applications, the second term of previous equation can be approximated by [8]

$$k_{eff}^2\frac{d}{dz}(k_{eff}^{-2}\frac{dq_c}{dz}) \approx \frac{d^2q_c}{dz^2} \tag{7}$$

Resulting in the final equation which is the basis for the derivation of the GFPE propagation model.

$$\frac{d^2q}{dr^2} + \frac{d^2q}{dz^2} + k^2q = 0 \tag{8}$$

3.2. Kirchhoff-Helmholtz integral equation

The two dimensional Kirchhoff-Helmholtz equation can be obtained assuming that the wave field P(r) is independent of the y coordinate [6]

$$P(r_A)=-\frac{1}{4\pi}\int_C[P(r)\nabla g_2(r,r_A)-g_2(r,r_A)\nabla P(r)]ndS \tag{9}$$

It is possible to rewrite the two dimensional Helmholtz equation by the following expression,

$$\nabla^2P(r) + k^2(r)P(r) = 0 \tag{10}$$

The integral known in acoustics as the Rayleigh II integral is expressed as

$$P(r_A) = \frac{1}{2\pi}\int_{-\infty}^{+\infty}(P(r)\frac{dg(r,r_A)}{dx})_{x=x_0}dz \tag{11}$$

A derivation of the governing equation of the GFPE method can be obtained by applying the residue theorem and manipulating the integrals in order to get a unique dependence on the wave number [8],

$$q(\Delta r + r, z) = \frac{1}{2\pi} \int_{-\infty}^{+\infty} e^{i\Delta r\sqrt{k_0^2 - k_z^2}} e^{ik_z z} dk_z \int_0^{+\infty} e^{-ik_z z'} q(r, z') dz' + \frac{1}{2\pi} \int_{-\infty}^{+\infty} R(K_z) e^{i\Delta r\sqrt{k_0^2 - k_z^2}} e^{ik_z z} dk_z \int_0^{+\infty} e^{ik_z z'} q(r, z') dz' + 2i\beta e^{-i\beta z} e^{i\Delta r\sqrt{k_0^2 - \beta^2}} \int_0^{+\infty} e^{-i\beta z'} q(r, z') dz' \quad (12)$$

The three terms of the right hand side of the equation above represents the sum of different types of sound waves. The first term represents the direct wave, the second term represents the wave reflected by the ground and the third term represents the surface wave. This is the applied equation for the Green's Function Parabolic Equation method.

4. Numerical Implementation

As the GFPE method is a step by step extrapolation of the sound field , a two dimensional rectangular grid is used, with two grid parameters (horizontal spacing and vertical spacing) depending on frequency. The length of the numerical grid is defined by the number of horizontal steps necessary to reproduce the horizontal distance between the source and the receiver.

4.1. Starting Field

It is used a Gaussian starting field defined as

$$q(0,z) = e^{\frac{-k_a^2 z^2}{B}} \sqrt{ik_a}(A_0 + A_2 k_a^2 z^2 + A_4 k_a^4 z^4 + A_6 k_a^6 z^6 + A_8 k_a^8 z^8) \quad (13)$$

where the coefficients A and B are dependent on the order of the Gaussian field and for convenience are presented on the following table

Order	A_0	A_2	A_4	A_6	A_8	B
0	1	0	0	0	0	2
2	1.3717	-0.3701	0	0	0	3
4	1.9705	-1.1685	0.0887	0	0	3
8	9.6982	-20.3785	6.0191	-0.4846	0.0105	3

Figure 1: Values of coefficients A and B

4.2. Artificial Absorption Layer

The discrete formulation of the governing equations requires a finite length of the atmosphere and consequently introduces unwanted and unrealistic reflections of sound waves at the top of the numerical grid.

This numerical error can be eliminated by introducing an artificial absorption layer at the top of the grid which attenuates the sound waves travelling upwards and reaching the maximum height discretized.

The implementation of such attenuation layer involves the manipulation of the wave number at the affected grid points by adding an imaginary part to its real value as follows,

$$k_{abs} = k(z) + i\alpha(z) \quad (14)$$

Where,

$$\alpha(z) = A\left(\frac{z - z_{abs}}{z_{top} - z_{abs}}\right)^2 \quad (15)$$

and A is a frequency dependent attenuation factor,z_{abs} is the initial height of the absorption layer and z_{top} is the maximum height of the numerical grid.

The absorption layer used has a thickness based on the wavelength of travelling sound waves and is typically delimited by 50λ and 100λ to avoid increasing the size of the Fourier transforms used in this propagation method.

4.3. Window Function

The window function acts like a numerical filter in k domain, suppressing the errors caused by the discrete sampling of the inverse Fourier Transform, without changing the value of the cumulative sum given by,

$$C(k_n) = \sum_{i=0}^{n} S(k_i) \quad (16)$$

The summand is multiplied by the window function to suppress its rapid oscillations

$$\begin{cases} 1, & |k| < 0.5K_a \\ cos^2(\frac{\pi(|k|-0.5k_a)}{k_a}), & 0.5k_a \leq |k| \leq k_a \\ 0, & |k| > k_a \end{cases} \quad (17)$$

4.4. Alternate Refraction Factor

In the Green's Function Parabolic Equation method, atmospheric refraction was taken into account by multiplying the solution by a exponential factor given by

$$e^{i\Delta r \delta k^2(z)} \quad (18)$$

4.5. GFPE's Validation

The following figure describes the three test cases, which have a non-refracting atmosphere, where the sound speed profiles for each test case are given by the following figure,

Test Case	1	2	3
Sound speed profiles	Homogeneous	Downward	Upward
Speed $c\ (m/s)$	$c = 343$	$c = 343 + z/10$	$c = 343 - z/10$

Figure 2: Sound speed profiles for each test case

For the simulation, were assumed three source frequencies and two different ranges for the observer: 10Hz, 100Hz and 1000Hz and considering a range of R=200m and R=2000m and the ground is assumed to be transversely uniform, to have range independent properties and to be a completely flat ground surface.

Ground Surface	Absorbing
$10\ Hz$	$Z_g = 38.79 + 38.41i$
$100\ Hz$	$Z_g = 12.81 + 11.62i$
$1000\ Hz$	$Z_g = 5.96 + 2.46i$
Source Height (m)	5
Receiver Height (m)	1

Figure 3: Ground parameters for the test cases

The ground impedance values are obtained with the following equation [1],

$$Z_g = \frac{w\rho_b}{k_b \rho_0 c_0} \quad (19)$$

Some of test case results are displayed below and were successfully compared to the benchmark results found in the literature [2]

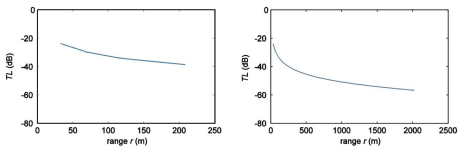

Figure 4: Transmission loss for 10Hz - Test case 1

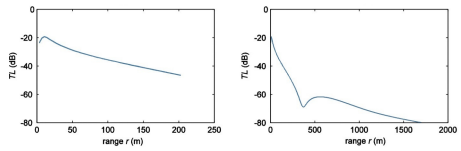

Figure 5: Transmission loss for 100Hz - Test case 1

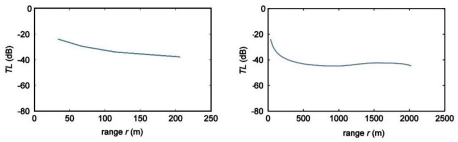

Figure 6: Transmission loss for 10Hz - Test case 2

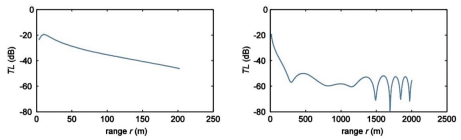

Figure 7: Transmission loss for 100Hz - Test case 2

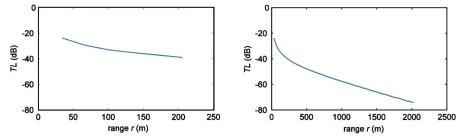

Figure 8: Transmission loss for 10Hz - Test case 3

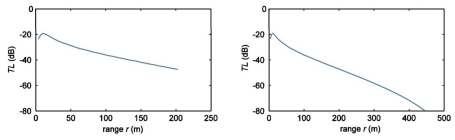

Figure 9: Transmission loss for 100Hz - Test case 3

5. ECAC Trajectory Model

Typically, modelling systems comprise three main elements, starting by an input of airport and aircraft data such as the runway heading and altitude and weather conditions, the aircraft's engines and flaps coefficients and a set of procedural steps to be modelled.This is followed by the application of the model, which processes the given input and converts it into an accurate and detailed flight path, which is then used to calculate the noise levels at the observer due to that flight departure. A briefly description of the steps in this process are the following:

1. Pre-Processing of Airport Data
2. Definition of Flight Path
3. Noise level at the observer

Having a trajectory defined by a sequence of points and the mentioned parameters at each of them, it is possible to start calculating noise levels received in different locations relatively to a single aircraft. The most common metrics used in modern aircraft noise indices are single-event sound exposure levels L_E which take into account all the sound energy in the events, and its exact values are given by the following equation,

$$L_E = 10\log(\frac{1}{t_0}\int_{t_1}^{t_2} 10^{\frac{L(t)}{10}}dt) \qquad (20)$$

Where t_0 corresponds to a reference time value, $L(t)$ is a noise level curve in function of time and $[t_1, t_2]$ is the time interval which should be chosen in such way that ensures that all the sound resulting from the event is comprised.

It is also used the metric L_{max} that is the maximum instantaneous level in the event.These two metrics will be calculated in this model in a different scale of noise, using the A-weighted filter to represent the human ear's sensitivity to different frequencies, resulting in the metrics L_{Amax} and L_{AE}. This last one can be obtained through the following expression,

$$L_{AE} = 10\log(\frac{1}{t_0}\int_{t_1}^{t_2} 10^{\frac{L_A(t)}{10}}dt) \qquad (21)$$

with $t_0 = 1$ second.

5.1. Coordinate System

It was necessary to define the coordinate systems to be used. With this in mind it was chosen a fixed local coordinate system with its origin at the Montijo's aerodrome track.

It was also necessary a one dimensional coordinate system which follows the ground track,where its axis is the ground track distance s and has its center on the start of roll in the runway in use. This will be the main system used while modelling the flight paths as it's specific for each ground track, representing a distance s measured along the track throughout the flight direction. In this system, any flight operation parameter is function of the distance s. For the scope of this thesis, all the distances refered to Montijo's Aerodrome used were measured acquired through Google Maps Tools.

A third and last reference system fixed to the aircraft will be used in situations where it's important to know the aircraft's position.

5.2. Aircraft Trajectory

The modeling approach presented in this thesis evaluates procedures to define a small set of trajectory model parameters. The model parameters are grouped according to typical phases of flight. It is in the scope of this thesis to calculate the trajectory of an aircraft departure, in which are included the following stages of a flight:

1. Take-off Roll
2. Take Off

3. Initial Climb
It was assumed changes of flight parameters between flight-phase events and all aircraft accelerations and decelerations were executed at a constant rate. Most flight phases defined here involve one speed transition where a new target airspeed is established at the beginning of a phase and maintained throughout the remainder of a phase [7].

5.3. Flight Profile
The parameters describing each flight profile segment at the start and end of the segment are:
s_1, s_2 distance along the runway
z_1, z_2 aircraft altitude
V_1, V_2 aircraft groundspeed
P_1, P_2 power parameter
ζ_1, ζ_2 bank angle

To build a flight profile from a set of procedural steps (flight path synthesis), segments are constructed in sequence to achieve required conditions at the end points[10]. The end-point parameters for each segment become the start-point parameters for the next segment.

In any segment calculation the parameters are known at the start; required conditions at the end are specified by the procedural step and the steps themselves are defined by the ANP database. The end conditions are usually height and speed and the profile building task is to determine the track distance covered in reaching those conditions.

The result is a sequence of co-ordinate sets (x, y, z), each being either a node of the segmented ground track, a node of the flight profile or both, the profile points being accompanied by the corresponding values of height z, ground speed V, bank angle ζ and engine power P.

5.4. Departure Flight Path
The script reads the information from the CSV datasheets from ANP Database refering to Airbus A320-211 with motors CFM565 and reads the parameters to execute the flight path segmentation. All the trajectories follow the procedural departure steps from ECAC Vol.II and simultaneously the flight path sugested by the NAV study [5] with 10% climb rate.

For the several simulated trajectories it was adopted a turning radius of 5.000ft (test case 1), 10.000ft (test case 2) and 20.000ft (test case 3) and for all and each one of them the climbing rate was constant.

It is generated a text file with the several coordinates (x, y, z) of the aircraft for the coordinate system framed in Montijo's groundtrack and also the absolute distance from the aircraft to the observer.

The the several trajectory plots for each test case are displayed below, with the interest zones PISCO and DANIL zones marked.

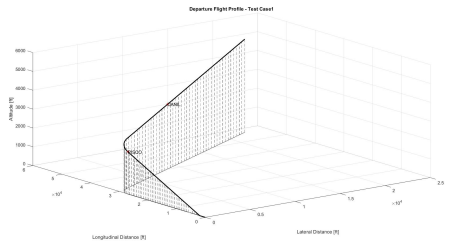

Figure 10: Flight path - Test case 1 with turning radius of 5.000ft

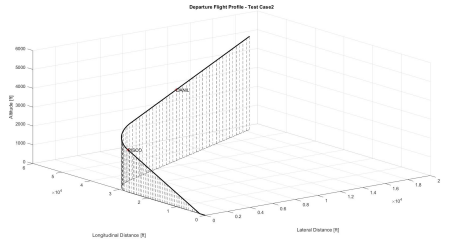

Figure 11: Flight path - Test case 2 with turning radius of 10.000ft

6. Noise Levels Results
The obtained noise levels are related to a fixed receiver located at EXPO woth coor-

dinates $38°46009.5"N 9°05032.9"W$ during the aircraft departure from Montijo.

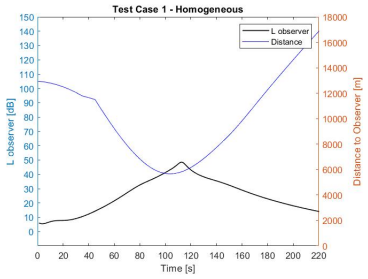

Figure 12: Test case 1 - Homogeneous

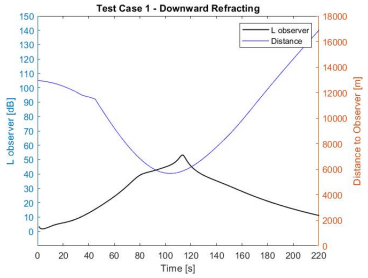

Figure 13: Test case 1 - Downward

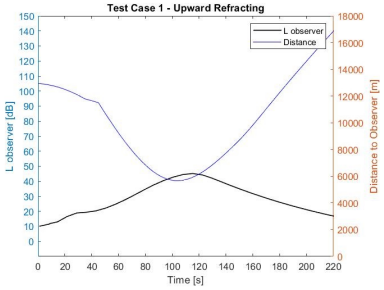

Figure 14: Test case 1 - Upward

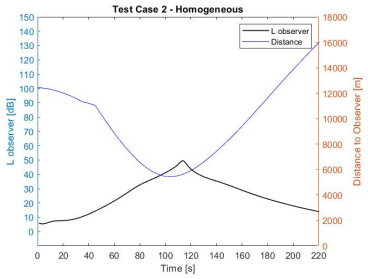

Figure 15: Test case 2 - Homogeneous

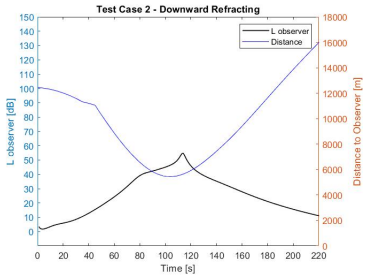

Figure 16: Test case 2 - Downward

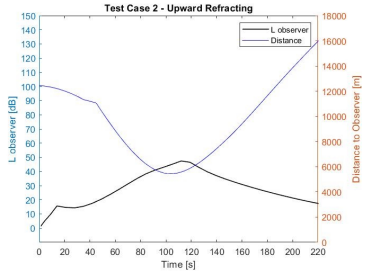

Figure 17: Test case 2 - Upward

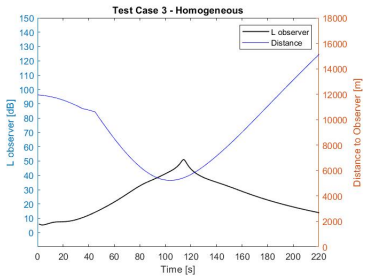

Figure 18: Test case 3 - Homogeneous

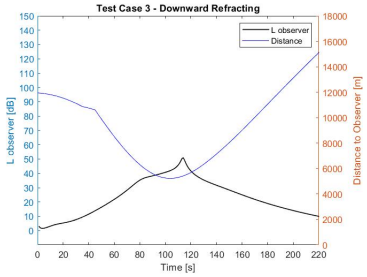

Figure 19: Test case 3 - Downward

The results suggest that there are very little differences for the three test case trajectorys and that is because the three have the turning zone situated at the same location in which the distance is minimum to the observer. This results in approximately the same range between the source and the re-

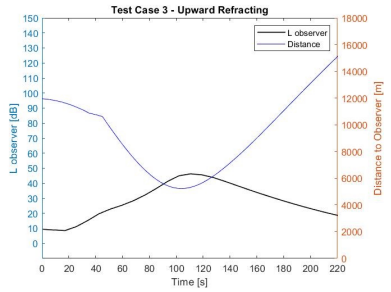

Figure 20: Test case 3 - Upward

ceiver and therefore it is not expected that the noise levels vary that much. We can also notice that the maximum noise levels at the observer have a similar evolution for the homogeneous and the downward refracting atmosphere and that is supported by the fact of the distance being large where the noise levels are not that much changed. Also for every plot we can see a displacement between the minimum distance and the maximum noise which has the value of the time that sound needs to propagate in the atmosphere. In other words, when the aircraft is at its nearest position from the receiver, it takes a certain time to travel and therefore the maximum noise level its just perceived at the receiver after a while, corresponding to the time that the sound takes to travel along the distance between them for a constant sound speed. In the test case 1 trajectory the maximum noise level at the observer is 50 dB for the homogeneous atmosphere while for the downward refracting atmosphere is 53 dB. This small change is due to the fact that the sound waves are bend downward through out its path and this allows to reach higher levels for the same travelled distance, however since the distance is very large the difference is very little and probably unnoticed by the observer. For the upward refracting atmosphere simulation the noise levels are more attenuated than in the other types and only reach a maximum level of approximately 46 dB with a much more smooth evolution along the time history. Therefore it is possible to conclude that an upward refracting atmosphere is better for attenuating noise levels generated by aircraft departures. For the test case 2 and 3 trajectorys the noise levels perceived by the observer are in the same range of values that the test case 1 and this suggests that the turning radius after the PISCO zone does not influence much the noise levels at the observer since that the difference of the distances between the observer and the source are very small when compared to the overall distance that the sound travels. From a practical point of view it is possible to claim that taking into account the predicted levels of noise at the specified observer, the Montijo's future airport won't generate significant levels of noise at the riverside zone of Lisbon since these noise levels are similar to those generated in a normal conversation. Taking into account that in this zone there is a considerable ammount of cars traffic and that it has a large train station where it is expected that the normal noise levels in this zone reach near 80 dB during the most busy hours, we can affirm that the noise generated by an aircraft departure is almost or totally unnoticed at the observer location.

Finally, the Sound Exposure Level (SEL), which accounts the integration of the SPL curve during the aricraft departure procedure, was obtained. As the relevant sound energy for the 10 dB down integration is concentrated around the maximum SPL value, only a small part of the aircraft's trajectory is considered in the calculations due to the rapid evolution of the SPL curve at the proximity of the maximum SPL value.

	Test Case 1		
	Homogeneous Atmosphere	Downward refracting	Upward refracting
SEL (L_{AE})	55.3 dB	57.8 dB	54.2 dB
L_{max}	49.5 dB(A)	53.9 dB(A)	46.7 dB

Figure 21: L_{AE} and L_{max} values for Test case 1

	Test Case 2		
	Homogeneous Atmosphere	Downward refracting	Upward refracting
SEL (L_{AE})	56.2 dB	58.8 dB	55.1 dB
L_{max}	51.3 dB(A)	54.4 dB(A)	47.9 dB

Figure 22: L_{AE} and L_{max} values for Test case 2

	Test Case 3		
	Homogeneous Atmosphere	Downward refracting	Upward refracting
SEL (L_{AE})	57.8 dB	59.1 dB	55.4 dB
L_{max}	51.9 dB(A)	54.8 dB(A)	48.4 dB

Figure 23: L_{AE} and L_{max} values for Test case 3

Conclusion

The results obtained in this thesis include multiple simplifications that should be considered, as for example the exclusion of turbulence and wind, however, for the purpose of this thesis, it was possible to take a notion of how much predicted impact the noise produced by an aircraft takes on a person while within a radius of considerable large distance. The obtained results made possible to take some conclusions, being briefly concluded that for an Airbus A320 with motors CFM565, a single individual would perceive a very low noise level during a Montijo's airbase departure, and therefore, the impact generated for the Oriente living zone is predicted to be insignificant when compared to the noise levels already existing.

For a more realistic and accurate study, several developments should be included as for example the consideration of a turbulent atmosphere and also atmospheric wind. The ground surface should be developed in detail in order to be possible to simulate noise barriers and other topographic features and obstacles, and should even be considered different ground materials not forgeting the aircraft cinematics, which also play a very important role, and which should be included with much more detail in the algorithm to allow to obtain a more realistic flight path.

References

[1] J. Cooper and D. Swanson. Parameter selection in the green's function parabolic equation. *Applied Acoustics*, 68:390–402, 04 2007.

[2] K. A. et al. Benchmark cases for outdoor sound propagation models. *The Journal of the Acoustical Society of America*, 97:173–191, 01 1995.

[3] A. F. Garcia Peixoto de Oliveira. The effect of wind and turbulence on sound propagation in the atmosphere. *Outdoor Propagation Acoustics*, 1:108, 06 2012.

[4] K. Gilbert and M. White. Application of the parabolic equation to sound propagation in a refracting atmosphere. *The Journal of the Acoustical Society of America*, 85:630–637, 02 1989.

[5] João Paulo Mendonça, Manuel Araújo. Estudo de Rotas Alternativas e Altitudes (LMPT)- Pistas 01 e 19, Novembro 2018.

[6] R. Korte and K. Gilbert. A fast green's function method for one-way sound propagation in the ocean. 95:2907–, 05 1994.

[7] R. Mayer. A flight trajectory model for a pc-based airspace analysis tool. 08 2003.

[8] E. M. Salomons. *Computational Atmospheric Acoustics*. Springer Netherlands, 1 edition, 2001.

[9] Scott MacDonald. Sound Transmission Loss - Determining the Acoustic Properties of Materials Solution Brief, oct 2019.

[10] O. Zaporozhets. *Aircraft Noise Models for Assessment of noise around Airports - Improvements and Limitations*, pages 50–55. 09 2016.